Computer Modeling in Engineering & Sciences

Tech Science Press

https://doi.org/10.32604/cmes.2026.088858

ARTICLE

A Load Identification Method for Bogie Frames: Improvement and Engineering Application

Bo Liu[1,2], Yuedong Wang[1,2], Jiaqi Zhang[1,2,*], Qi Dong[1,2], Qiyu An[1,2], Tao Guo[1,3], Guojie Cai[1,3] and Yawen Fu[4]

[1]Zhan Tianyou College (CRRC College), Dalian Jiaotong University, Dalian, China
[2]Key Laboratory of Railway Industry on Safety Service Key Technologies for High-Speed Train, Dalian Jiaotong University, Dalian, China
[3]Bogie Technology Centre, CRRC Tangshan Co., Ltd., Tangshan, China
[4]Dalian Wanhe Testing Technology Co., Ltd., Dalian, China

*Corresponding Author: Jiaqi Zhang. Email: zhangjq@djtu.edu.cn

Received: 10 July 2026; Accepted: 23 September 2026; Published: 21 October 2026

ABSTRACT: As the key load-bearing structure of railway vehicles, the bogie frame plays a critical role in operation. The identification of operating loads for the bogie frame constitutes an essential part of structural design and safety assessment. An improved method based on standard Tikhonov regularization is proposed by combining intelligent algorithms and physical models, to address the issue that weakly correlated loads associated with small singular values are considerably susceptible to noise interference in bogie frame load identification. A systematic procedure for bogie frames, integrating load identification, finite element simulation and fatigue assessment, is established. This method introduces a non-identity matrix constructed from the singular values of the transfer coefficient matrix, and adopts a genetic algorithm to achieve adaptive parameter selection. Minor corrections are applied to large singular values associated with strongly correlated loads, while the correction magnitude for small singular values of weakly correlated loads that are sensitive to noise is increased. Subsequently, load identification verification is performed on the bogie frame, and the average relative error is significantly reduced. Furthermore, the accuracy of the proposed method is validated using field measurement data of a new-type bogie frame with inner axle-boxes. Finally, the integrated "load identification–finite element simulation–fatigue assessment" procedure in this study is implemented as visualization software and applied to the aforementioned new-type bogie frame. This study provides a numerical solution for load identification and offers conservative load inputs for finite element modeling and fatigue strength analysis of bogie frames.

KEYWORDS: Tikhonov regularization; load identification; bogie frame; ill-conditioned matrix; fatigue life

1 Introduction

The bogie frame is a key load-bearing and operational component in the running gear of railway vehicles, and the reliability of its structural strength is directly linked to the operational safety of the vehicle. At present, China has established an independent research and development capacity for railway vehicles and mastered relevant core technologies, whereas the design loads of bogie frames are still formulated in accordance with international standards [1,2]. Design standards are inconsistent with actual operating conditions, and considerable deviations are found between in-service operating loads and standard design loads, which leads to inaccurate strength design of vehicle bogie frames [3–5]. Therefore, the reliability of

Copyright © 2026 The Authors. Published by Tech Science Press. This work is licensed under a Creative Commons Attribution 4.0 International License, which permits unrestricted use, distribution, and reproduction in any medium, provided the original work is properly cited.

strength evaluation in the structural design phase of railway vehicles can be effectively improved through research on load identification methods for bogie frames.

In the field of railway vehicle load research, Zhu et al. [6] propose an analytical method for wheel-rail force identification based on structural dynamics theory, by applying the Duhamel integral and incorporating the characteristics of railway vehicle systems. Subsequently, vertical wheel-rail force identification is investigated by Zhu et al. [7] on the basis of the time-domain method, combined with a machine learning-based correction strategy. A radial load identification model is constructed by Ren et al. [8] using a serial deep neural network composed of a one-dimensional convolutional neural network and a bidirectional gated recurrent unit, and hyperparameter optimization of the model is achieved by adopting the Hyperband algorithm. To address the insufficient accuracy of the traditional quasi-static method when the excitation frequency approaches the natural frequency of the frame, Lu et al. [9] introduce a correction strategy based on reference point stresses and propose a load identification method suitable for metro vehicle bogie frames. In the engineering domain of railway vehicles, data-driven methods including machine learning [10] and neural networks [11] are widely regarded as major current research hotspots. However, such methods have inherent limitations, such as high reliance on high-quality training data and constrained generalization performance. Therefore, in the engineering practice of bogie frame load identification, traditional regularization methods still retain significant value due to their merits of concise theoretical framework and clear engineering interpretability.

Regularization methods are effective approaches to handle ill-posed problems. The basic idea is that a set of regularized solutions can be obtained by imposing appropriate additional conditions or boundary constraints, and the solution that best matches the governing equation can be selected from the set [12,13]. To solve the ill-posed problems in the inversion process of structural dynamic loads, the optimal parameters are obtained by Xi et al. [14] using a micro-population genetic algorithm, and ill-conditioned problems such as matrix inversion are avoided. The Tikhonov regularization method is extended by Pacheco et al. [15] through generalized singular value decomposition, so that it can be applied to regularization problems of arbitrary order. A regularization parameter selection strategy based on the A-optimal design method is proposed by Wang and Gu [16] and applied to the inversion of seismic slip distribution. These studies provide theoretical, numerical and practical guidance for load identification in multiple fields. However, in the current load identification of railway vehicles, the theoretical system of establishing differentiated regularization parameter selection strategies based on load correlation remains incomplete. Considering that singular values of different magnitudes in the frequency response function matrix have different effects on the stability of identification results, an improved regularization method is proposed by Jing et al. [17] on the basis of the inverse virtual excitation method. The effectiveness of this method is verified through multi-point stationary random load tests on simply supported beams.

Structural strength assessment based on identified dynamic loads is of great importance for ensuring the safe operation of bogie frames. Xiu et al. [18] find that the loads specified in international standards are conservative, and the application of field-measured loads to the structural design phase involves lengthy simulation computations. Wang et al. [19] develop a high-precision force-measuring frame for long-term on-track tests to obtain the actual loading conditions and damage states at fatigue-critical locations. Different from the design loads specified in international standards, Yin et al. [20] determine the optimal calibration coefficient for each load amplitude using a calibration method based on the damage consistency criterion, and establish a damage-consistent test load spectrum to realize fatigue damage prediction under actual service conditions. Li et al. [21] reconstruct the load phase information lost during rainflow counting through bench loading tests, build a load-prediction stress model with a phase matrix, and evaluate the structural damage state via equivalent stress. Most of the above studies rely on field measurement data, yet the

acquisition of field-measured response data involves a complex process. Therefore, load reconstruction based on measured signals in existing studies is inevitably affected by measurement noise [22,23]. Meanwhile, traditional fatigue assessment procedures suffer from cumbersome operations and redundant steps. Massive data computations tend to cause deviations between load identification results and fatigue assessment outcomes.

Weakly correlated loads corresponding to small singular values are highly susceptible to noise interference during the load identification process of bogie frames. An improved method based on standard Tikhonov regularization is proposed by combining intelligent algorithms with physical models, and a systematic procedure from load identification to fatigue assessment is established for bogie frames. This method introduces a non-identity matrix constructed from the singular values of the transfer coefficient matrix and adopts a genetic algorithm for adaptive parameter selection. Minor corrections are applied to large singular values associated with strongly correlated loads, while the correction magnitude for small singular values corresponding to weakly correlated loads that are sensitive to noise is increased. Through such differentiated processing of response data, the accuracy of bogie frame load identification is improved. Subsequently, load identification verification is conducted on bogie frames, and the average relative error is significantly reduced. Furthermore, the accuracy of the proposed method is further validated with field measurement data of a new-type bogie frame with inner axle-boxes. Finally, the integrated "load identification-fatigue assessment" procedure developed in this study is implemented as visualization software and applied to the aforementioned new-type bogie frame. This study provides a solution for bogie frame load identification and is of great value to the structural strength design and safety assessment of railway vehicles.

In summary, the contributions of this paper are:

(1) An improved Tikhonov regularization method with differentiated processing of measured response data;
(2) Field measurement of the new-type bogie frame with inner axle-boxes;
(3) The integrated "load identification-fatigue assessment" procedure and visualization software based on measured data.

2 Method

2.1 Singular Value Decomposition

The key to solving ill-posed problems with regularization methods lies in constructing a proper regularization operator, and all common methods for constructing regularization operators are established on the basis of singular value decomposition (SVD) theory [24].

For a linear time-invariant system, its dynamic load identification system model is expressed as:

$$\boldsymbol{b} = \boldsymbol{A}\boldsymbol{x} \tag{1}$$

where $\boldsymbol{b}$ is the $m \times 1$ measurement response matrix, $\boldsymbol{x}$ is the $n \times 1$ load matrix, and $\boldsymbol{A}$ is the $m \times n$ load transfer coefficient matrix, where m is the number of measurement responses and n is the number of unknown loads.

In engineering applications, the transfer coefficient matrix $\boldsymbol{A}$ is usually ill-conditioned. By performing SVD on matrix $\boldsymbol{A}$, the matrix is rewritten as:

$$\boldsymbol{A} = \boldsymbol{U}\boldsymbol{\Sigma}\boldsymbol{V}^{\mathrm{T}} = \sum_{i=1}^{n} u_i \sigma_i v_i^{\mathrm{T}} \tag{2}$$

where $\boldsymbol{U} = (u_1, \ldots, u_m)$ and $\boldsymbol{V} = (v_1, \ldots, v_n)$ denote the $m \times m$ and $n \times n$ orthogonal matrices, respectively. u_i and v_i are the eigenvectors obtained from $\boldsymbol{A}\boldsymbol{A}^{\mathrm{T}}$ and $\boldsymbol{A}^{\mathrm{T}}\boldsymbol{A}$, respectively. $\boldsymbol{\Sigma} = diag(\sigma_1, \ldots, \sigma_n)$ denotes the

diagonal matrix constructed from the singular values, where σ_i is the singular values of matrix $\boldsymbol{A}$, and let $\sigma_1 \geq \cdots \geq \sigma_n \geq 0$.

Combined with the singular value decomposition method, Eq. (1) is solved and the result $\boldsymbol{x}_{SVD}$ is given as:

$$\boldsymbol{x}_{SVD} = \boldsymbol{V}\boldsymbol{\Sigma}^{-1}\boldsymbol{U}^{\mathrm{T}}\boldsymbol{b} = \sum_{i=1}^{n} \frac{u_i^{\mathrm{T}}\boldsymbol{b}}{\sigma_i} v_i \tag{3}$$

In load identification, the condition number is commonly used as the criterion to evaluate the ill-conditioning of a matrix. For matrix $\boldsymbol{A}$, its condition number is defined as:

$$cond\,(\boldsymbol{A}) = \|\boldsymbol{A}\| \left\|\boldsymbol{A}^{-1}\right\| = \frac{\sigma_1}{\sigma_n} \tag{4}$$

The larger the condition number of a matrix, the more severe its ill-conditioning, and the lower the accuracy of $\boldsymbol{x}_{SVD}$ obtained by the singular value decomposition method [25]. To improve the accuracy of $\boldsymbol{x}_{SVD}$, the Tikhonov regularization method is widely adopted to mitigate the ill-conditioning of the transfer coefficient matrix.

2.2 Standard Tikhonov Method

The basic idea of the Tikhonov method is to introduce a regularization term into the objective function of the least squares method, so as to transform the linear problem into an optimization problem. The objective function optimized by the Tikhonov regularization method is expressed as:

$$\min \|\boldsymbol{A}\boldsymbol{x} - \boldsymbol{b}\|_2^2 + \lambda \|\boldsymbol{L}\boldsymbol{x}\|_2^2 \tag{5}$$

where λ is the regularization parameter and used to balance the residual norm and the solution norm, $\boldsymbol{L}$ is the regularization matrix, $\|\cdot\|_2^2$ denotes the squared two-norm of the parameter.

The least squares solution of the optimization problem satisfies:

$$\boldsymbol{x} = \left(\boldsymbol{A}^{\mathrm{T}}\boldsymbol{A} + \lambda \boldsymbol{L}^{\mathrm{T}}\boldsymbol{L}\right)^{-1} \quad \boldsymbol{A}^{\mathrm{T}}\boldsymbol{b} \tag{6}$$

SVD is performed on the coefficient matrix $\boldsymbol{A}$ and the regularization matrix $\boldsymbol{L}$. After rearrangement, the Tikhonov regularized solution can be obtained as:

$$\boldsymbol{x} = \sum_{i=1}^{n} \frac{\sigma_i^2}{\sigma_i^2 + \lambda\gamma_i^2} \frac{u_i^{\mathrm{T}}\boldsymbol{b}}{\sigma_i} v_i = \sum_{i=1}^{n} f \frac{u_i^{\mathrm{T}}\boldsymbol{b}}{\sigma_i} v_i \tag{7}$$

where $\boldsymbol{\gamma}_1 \geq \cdots \geq \boldsymbol{\gamma}_n \geq 0$ represent the singular values obtained from the singular value decomposition of the regularization matrix $\boldsymbol{L}$. f denotes the filter function, which is expressed as $f = \sigma_i^2 / \left(\sigma_i^2 + \lambda\gamma_i^2\right)$.

In standard Tikhonov regularization, the regularization matrix $\boldsymbol{L}$ is usually set as the identity matrix $\boldsymbol{I}$, where $\boldsymbol{L} = \boldsymbol{I}$. In this case, the expression $\boldsymbol{\gamma}_1 = \boldsymbol{\gamma}_2 = \cdots = \boldsymbol{\gamma}_n = 1$.

Therefore, the standard Tikhonov regularized solution is written as:

$$\boldsymbol{x} = \sum_{i=1}^{n} \frac{\sigma_i^2}{\sigma_i^2 + \lambda} \frac{u_i^{\mathrm{T}}\boldsymbol{b}}{\sigma_i} v_i = \sum_{i=1}^{n} f \frac{u_i^{\mathrm{T}}\boldsymbol{b}}{\sigma_i} v_i \tag{8}$$

The filter function corresponding to the standard Tikhonov regularization method is given by $f = \sigma_i^2 / \left(\sigma_i^2 + \lambda\right)$. An analysis of the characteristics of the filter function f shows that f approaches 1 for large

singular values, while $f < 1$ for small singular values. Thus, the differentiated correction of singular values can be realized by modifying the filter function f.

2.3 Improved Tikhonov Method

Although the Tikhonov regularization achieves a certain improvement in accuracy compared with the SVD, it gives rise to the problem of over-smoothing approximation in the objective function. This is attributed to the fact that the regularization matrix $\boldsymbol{L}$ in the standard Tikhonov regularization is an identity matrix. When processing the singular values of matrix $\boldsymbol{A}$, corrections of the same magnitude are applied to all singular values, and this strategy has obvious shortcomings. On one hand, it overcorrects the signals corresponding to large singular values. As the major components of the matrix, these signals have good noise immunity and their original information ought to be retained. On the other hand, it under corrects the signals associated with small singular values. Such signals are sensitive to noise and should be emphatically corrected during the regularization process. The standard Tikhonov method fails to effectively handle the differences in noise sensitivity among singular values.

Therefore, a non-identity matrix is introduced to impose minor corrections on large singular values and strengthen the correction magnitude for small singular values, so that the influence of noise is effectively suppressed. The proposed method improves the standard Tikhonov regularization and realizes differentiated corrections for different eigenvalues of the matrix by constructing a new diagonal regularization matrix.

For the selection of the regularization matrix, Jing et al. [17] improved the standard Tikhonov regularization by constructing a regularization matrix with diagonal elements of $\sqrt[4]{\sigma_1/\sigma_i}$. It can be concluded that proper selection of diagonal elements helps balance the sensitivity of different singular values to ill-posed problems. However, the matrix used is essentially an empirical parameter matrix. Its values lack support from physical principles, and its optimality has not been verified. Thus, in current engineering applications, this matrix can only be treated as a suboptimal approximate solution rather than an optimal engineering solution. Therefore, an improved Tikhonov regularization matrix based on the above matrix is proposed, with its diagonal elements denoted as $\boldsymbol{\gamma}_i$.

$$\boldsymbol{\gamma}_i = \sqrt[\alpha]{\frac{\sigma_1}{\sigma_i}} \tag{9}$$

where α is defined as both a power adjustment parameter and a non-negative variable, which is employed to regulate the intensity of the differentiated constraint.

The expression of the improved Tikhonov regularization matrix is given as:

$$\boldsymbol{L_I} = \begin{bmatrix} \sqrt[\alpha]{\frac{\sigma_1}{\sigma_1}} & 0 & \cdots & 0 & \cdots & \cdots & 0 \\ 0 & \sqrt[\alpha]{\frac{\sigma_1}{\sigma_2}} & 0 & \cdots & \cdots & \cdots & 0 \\ \vdots & \vdots & \vdots & \vdots & \vdots & \vdots & \vdots \\ 0 & 0 & \cdots & \sqrt[\alpha]{\frac{\sigma_1}{\sigma_m}} & 0 & \cdots & 0 \end{bmatrix}_{m \times n} \tag{10}$$

The improved regularized solution x_λ of the improved Tikhonov regularization matrix can be expressed as:

$$\boldsymbol{x}_\lambda = \sum_{i=1}^{n} \frac{\sigma_i^2}{\sigma_i^2 + \lambda \gamma_i^2} \frac{u_i^T \boldsymbol{b}}{\sigma_i} v_i = \sum_{i=1}^{n} \frac{\sigma_i^2}{\sigma_i^2 + \lambda \sqrt[\alpha]{\left(\frac{\sigma_1}{\sigma_i}\right)^2}} \frac{u_i^T \boldsymbol{b}}{\sigma_i} v_i \tag{11}$$

A large volume of on-track measurement data is required to be processed for a single evaluation of the objective function in this study. Accordingly, the selection of optimization algorithms shall satisfy the requirements for both computational cost and the stability of global optimality. Among conventional approaches, grid search is a uniform traversal method. While it is deemed straightforward in single-parameter scenarios, its computational efficiency is extremely low when large-scale datasets are involved. As a typical swarm intelligence algorithm, particle swarm optimization can achieve fast convergence when applied to low-dimensional unimodal functions. However, measurement noise and random fluctuations are present in on-track test data, by which the performance of particle swarm optimization is considerably affected [26]. The genetic algorithm is an optimization algorithm that searches for the optimal solution by simulating the process of natural evolution, and possesses strong global optimization capability. An adaptive genetic algorithm is adopted for the solution of α, and the specific steps of the algorithm are as follows [27]: In the initialization phase, parameter setting, chromosome encoding and random population generation are completed. During each iteration, the algorithm calculates the individual fitness and the average fitness of the whole population. The population is divided into groups according to the iteration count, and an elitist preservation strategy is applied to retain the optimal individuals for the next generation. Crossover and mutation operations are controlled based on the formula of adaptive crossover and mutation probability, with differentiated strategies implemented for population groups at different fitness levels. The algorithm adopts single-point crossover and swap mutation for high-fitness populations, while multi-point crossover and inversion mutation are used for low-fitness populations. After each iteration, the optimized sub-populations are reintegrated. The algorithm determines whether to continue the evolution process by checking if the maximum number of iterations is reached.

In load identification, identification accuracy serves as the most important evaluation criterion; therefore, the adaptive genetic algorithm is adopted to solve for the parameter α. The genetic algorithm selects α by minimizing the mean relative error (MRE).

$$MRE = \frac{1}{n} \sum_{i=1}^{n} \left| \frac{x_i - \hat{x}_i}{x_i} \right| \tag{12}$$

where x_i is the true load and $\hat{x}_i$ is the predicted value obtained from load identification.

The genetic algorithm is applied to the load identification of bogie frames, and the global optimal solution of α is obtained by taking the minimization of relative identification error as the objective function. When the ill-conditioning degree of the matrix is relatively high, analysis on the regularization matrix $\boldsymbol{L_I}$ shows that the singular values γ_i of $\boldsymbol{L_I}$ are significantly correlated with the singular values σ_i. When σ_i is large, the value of γ_i approaches 1, which results in a small correction magnitude for the principal component signals and thus avoids over-correction. As σ_i decreases, γ_i shows an increasing trend, which strengthens the correction magnitude for noise-sensitive signals and suppresses the influence of noise.

The selection of the regularization parameter λ is also critical, as it controls the balance between data fitting and the smoothness of the solution. In this paper, the generalized cross-validation (GCV) criterion is adopted to determine the optimal regularization parameter. The GCV criterion automatically selects the

optimal regularization parameter λ by minimizing an approximation of the prediction error, and its objective function is expressed as:

$$\mathrm{GCV}(\lambda) = \frac{\|\boldsymbol{A}\boldsymbol{x}_\lambda - \boldsymbol{b}\|_2^2}{\left[\mathrm{Trace}\left(\boldsymbol{I} - \boldsymbol{A}\left(\boldsymbol{A}^{\mathrm{T}}\boldsymbol{A} + \lambda \boldsymbol{L}^{\mathrm{T}}\boldsymbol{L}\right)\right)\right]^2} \tag{13}$$

where $\boldsymbol{x}_\lambda$ represents the regularized solution, and Trace in the denominator denotes the trace of the matrix.

The load identification procedure of the improved Tikhonov regularization method is illustrated in Fig. 1.

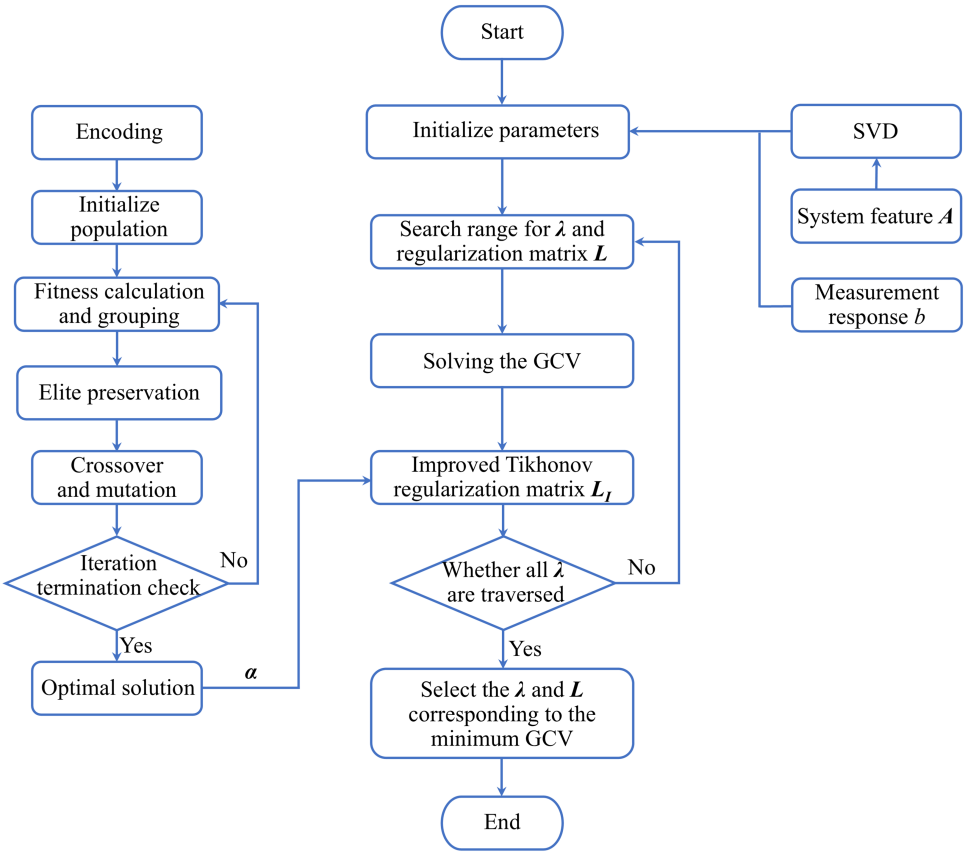


Figure 1: Procedure of the improved Tikhonov regularization method.

2.4 Fatigue Assessment Procedure Based on Load Identification Results

The loads acting on railway vehicles during service are complex and variable under environmental influences, and multiple load directions must be considered in structural stress calculation. In actual service, the bogie frame is subjected to complex multiaxial loads induced by wheel-rail coupling excitations and remains in a triaxial stress state. Therefore, a scientific conversion mechanism from multiaxial stress to uniaxial stress is required [28]. Existing studies that equate multiaxial problems to a uniaxial state based on static strength theory and then perform analysis via uniaxial fatigue theory are only applicable to multiaxial fatigue scenarios under proportional loading. However, the bogie frame is mostly subjected to non-proportional loads during train operation, especially non-proportional variable-amplitude loads. Under such conditions, uniaxial fatigue theory cannot deliver accurate assessment results, and relevant research

must be carried out based on multiaxial fatigue theory. Currently, the main approaches for converting multiaxial stress to uniaxial stress include the direct method and the projection method. The direct method compares stress magnitudes directly without considering stress directions. It identifies the maximum and minimum values among all principal stresses at a node to calculate stress amplitude and mean stress. This method features simple calculation, but it introduces errors by ignoring the vector nature of stress. The projection method, proposed by the European Rail Research Institute, is the most widely applied method in engineering practice [29,30]. This method follows the structural characteristic that fatigue crack initiation direction is perpendicular to the direction of maximum principal stress. It projects stresses in all directions onto the direction of maximum principal stress, realizing the conversion from a triaxial stress state to a uniaxial stress state.

Converting the multiaxial stress state to uniaxial stress via the projection method can more accurately reveal the mechanical factors leading to structural fatigue failure, which conforms to the fatigue failure mechanism under complex stress states. The Goodman criterion establishes a safety boundary in the stress amplitude-mean stress coordinate system, enabling intuitive judgment of the fatigue safety of a given stress state. Therefore, based on the measurement data, conducting load identification and performing fatigue assessment is of great significance for the structural design of the bogie frame. The integrated "load identification-fatigue assessment" procedure is illustrated in Fig. 2.

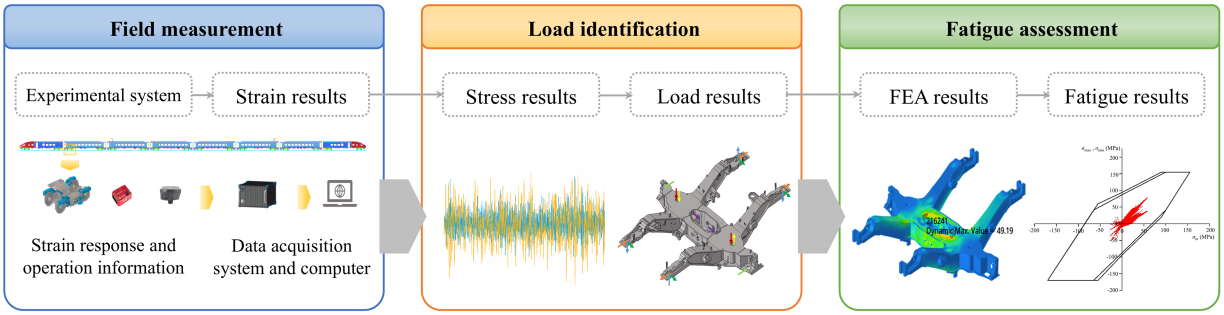


Figure 2: Procedure of the fatigue assessment.

3 Experimental Procedure

3.1 Field Measurement

Field measurements are conducted on the bogies of a certain type of electric multiple unit (EMU) equipped with inner axle-boxes. According to the load specifications given in the EN 13749 standard [31] and current research [32], the loads acting on the frame are divided into seven load systems, as shown in Fig. 3. Measuring points that are sensitive to individual loads and produce sufficiently large stress responses are selected as load identification points. After comprehensive consideration, seven stress measuring points are determined, and the load–stress transfer coefficients are calibrated on the test bench. The layout of these measuring points on the frame is presented in Fig. 4.

The total length of the experiment line is approximately 106.884 km, with the experimental speed incrementally increased from 180 to 250 km/h. This field measurement employs the digital signal acquisition system from IMC GmbH of Germany. This system features high data acquisition accuracy and strong anti-interference capabilities, enabling unattended, long-term continuous data collection, making it well-suited for field measurement. The sampling frequency for all measurement points in the experiment is set to 1000 Hz, achieving a balance between data acquisition accuracy and the volume of collected data [33]. The experimental system configuration is shown in Fig. 5.

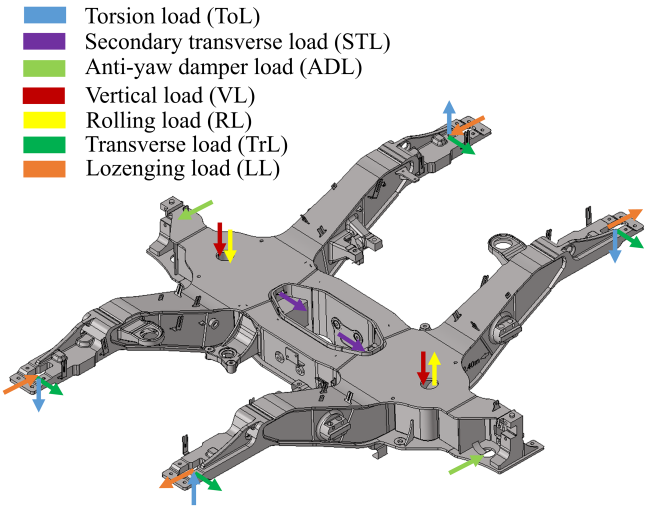


Figure 3: Frame load systems.

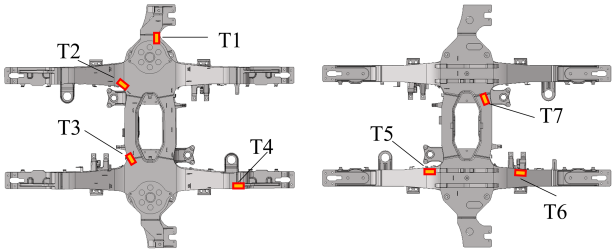


Figure 4: Layout of measuring points.

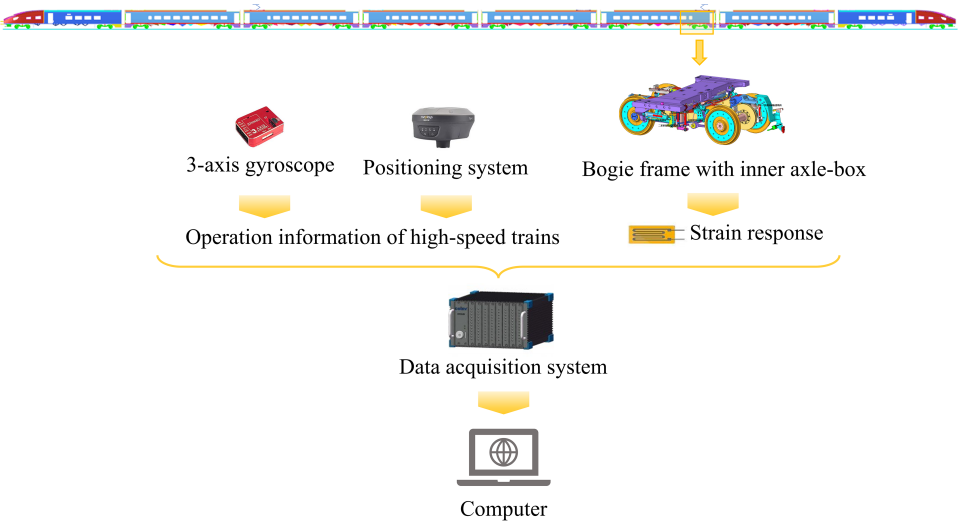


Figure 5: Experimental system.

Zero drift caused by temperature changes must be eliminated. Power line interference caused by periodic electromagnetic signals must be eliminated [34]. A section of data, which is 1900 s long and represents the

response signal at a running speed of 250 km/h, is selected for processing. After data processing including glitch elimination, zero drift removal and filtering, the field measured results are obtained as shown in Fig. 6.

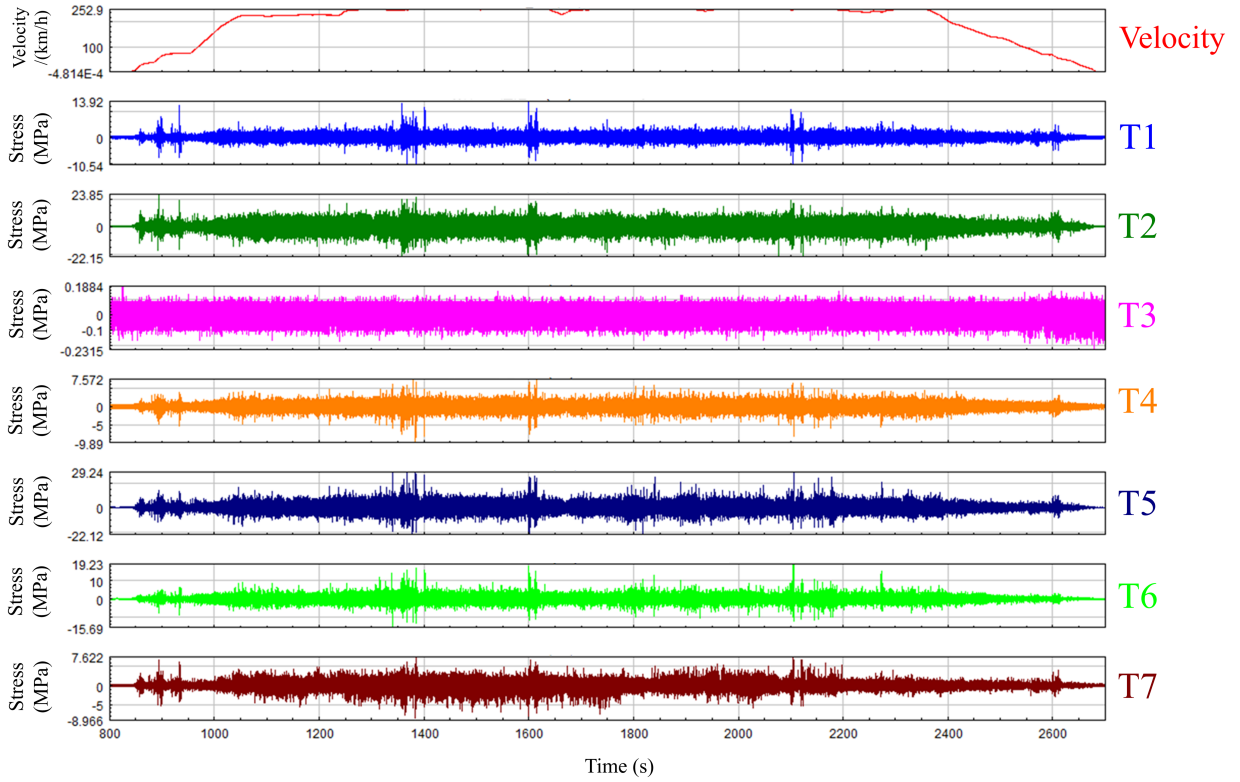


Figure 6: Experimental results.

3.2 Material Performance Test

The bogie frame is fabricated from S355J2W+N steel. To accurately establish the correlation between strain data and stress data, samples are taken from the in-service bogie frame. Tensile specimens are prepared in accordance with GB/T 228.1-2021 [35], and the material properties of the in-service bogie frame are tested using a universal testing machine. During the test, the control system of the testing machine acquires force values and corresponding specimen elongation data in real time. These data are transmitted to the supporting computer software for recording and processing. As the tensile force increases continuously, the specimen deforms progressively until fracture occurs, at which point the test is concluded. The test device and results are presented in Figs. 7 and 8, respectively.

Test results show that the material exhibits no obvious yield plateau and features continuous yielding behavior. Similar to conventional metallic materials, it is a strain-rate hardening material, whose yield strength increases with rising strain rate. However, this study focuses on the conversion relationship between strain and stress data, so the slope value of the elastic stage needs to be explicitly determined. The elastic modulus is determined as 206,000 MPa by averaging the test results of different specimens.

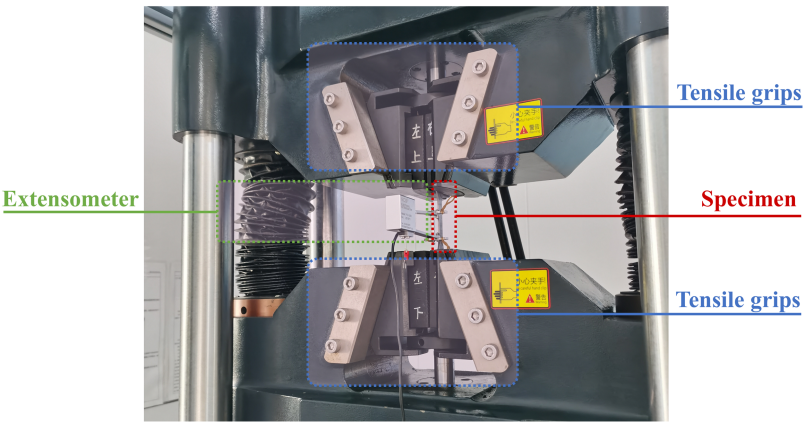


Figure 7: Material testing device.

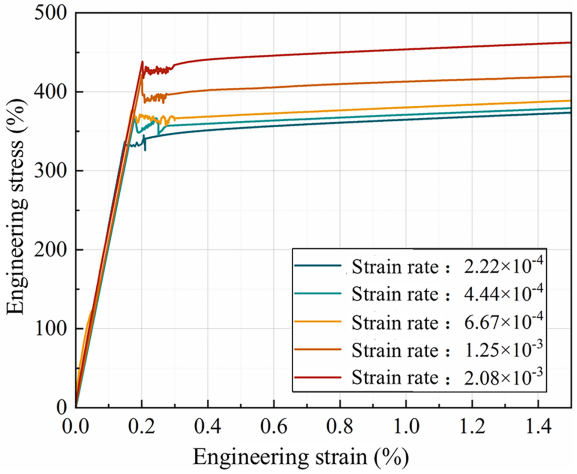


Figure 8: Stress-strain test results.

4 Validation

4.1 Method Validation

The correlation between applied loads and structural responses is determined by the transfer coefficient matrix. The improved method is developed on the basis of the singular values derived from the transfer coefficient matrix. Different levels of Gaussian noise are artificially introduced to examine the anti-interference capability of the proposed algorithm under varying noise levels. A feasibility study on load identification based on regularization methods is conducted for the bogie frame of the aforementioned EMU. The load data are normalized, with all loads set to a value of 1. The measured response under ideal conditions is calculated according to Eq. (1). Gaussian noise of 5%, 10% and 20% is separately added to the measured response to simulate the actual measurement environment. The load identification performance of the standard Tikhonov regularization method and the improved Tikhonov method is then analyzed under different noise levels. To quantify the error between the calculated loads and the true loads, *MRE*, relative error (*RE*) and standard deviation (*SD*) of each estimated value are compared, so as to evaluate the stability of the improved method.

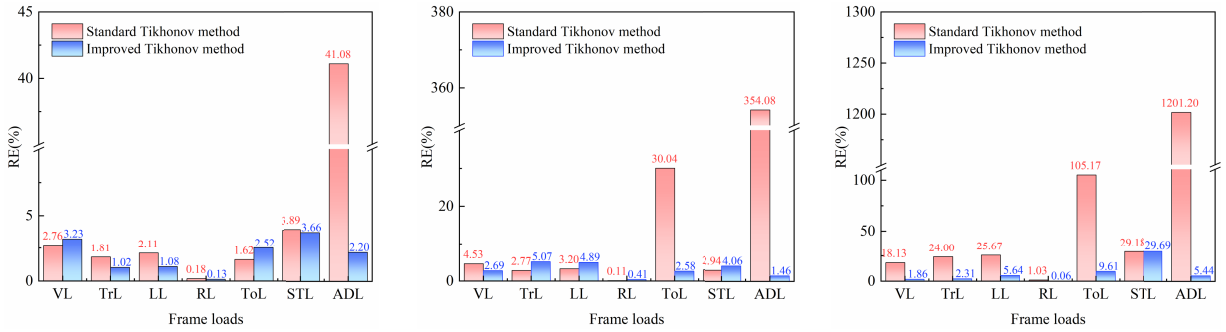
$$RE = \left| \frac{x_i - \hat{x}_i}{x_i} \right| \tag{14}$$

$$SD = \sqrt{\sum_{i=1}^{n} \frac{(\hat{x}_i - \overline{x}_i)^2}{n}} \tag{15}$$

where $\overline{x}_i$ represents the mean of the predicted values from load identification.

In the improved Tikhonov method, the optimal value obtained by the genetic algorithm with population grouping strategy and adaptive population proportion variation is 2.97.

The relative identification errors of the two regularization methods under different noise levels are shown in Fig. 9. The standard Tikhonov regularization method yields relatively accurate results for most load identifications, but shows poor accuracy for some loads, such as the load of the secondary transverse damper. Analysis indicates that the load-stress transfer coefficients of these loads are small, and their corresponding singular values are also small. This means the load-stress correlation is weak and more sensitive to noise, which leads to deviations in the load identification results. When identifying dynamic loads using the time-domain method based on physical models, weak correlation between partial loads and measuring points is unavoidable due to various factors, including incomplete response observation and limited strain gauge placement caused by structural constraints. Therefore, it is necessary to improve the load identification for weakly correlated measuring points.



(a) 5% Gaussian noise (b) 10% Gaussian noise (c) 20% Gaussian noise

Figure 9: Comparative analysis of relative errors.

On the basis of ensuring the identification accuracy of the first six loads, the improved method focuses on optimizing the correction of loads corresponding to small singular values. The results demonstrate that this method significantly improves the identification accuracy of the transverse load of the motor mount and the longitudinal traction load, and greatly reduces the identification errors. In particular, the improvement effect on the load identification of the secondary transverse damper is more prominent.

Table 1 presents the *SD* and *MRE* of the two regularization methods under different noise levels, respectively. Compared with the standard Tikhonov method, both the standard deviation and the mean relative error of the improved algorithm are significantly reduced. At the 5% noise level, the improved method shows only a minor improvement over the standard Tikhonov method. As the noise level increases, the improvement effect of the proposed method becomes increasingly significant.

The results show that, for the bogie frame of this type of EMU, the improved Tikhonov regularization method achieves high identification accuracy when is used as the regularization matrix, and can yield solutions with smaller errors and better stability.

Table 1: Comparative analysis of standard deviations and mean relative errors.

Noise Level	Method	*SD*	*MRE*
5%	Standard Tikhonov method	0.0247	0.54%
	Improved Tikhonov method	0.0073	0.52%
10%	Standard Tikhonov method	0.0383	2.43%
	Improved Tikhonov method	0.0241	1.72%
20%	Standard Tikhonov method	0.0407	2.22%
	Improved Tikhonov method	0.0288	1.95%

In practical on-track measurements, load identification results can be affected by zero drift, power line interference, spike glitches and other uncertainties. Accordingly, preprocessing steps including de-spiking, drift removal and band-stop filtering are commonly implemented on strain signals in the signal processing procedure. To demonstrate the impact of practical engineering noise and enable comparative analysis, a segment of test data is selected for analysis. For this dataset, only zero drift correction is performed on the raw signal, with all other noise components retained without filtering. The improved Tikhonov regularization method is adopted for calculation. Taking the vertical load as an example, the load identification results obtained from the raw data and the denoised data are compared, as illustrated in Fig. 10.

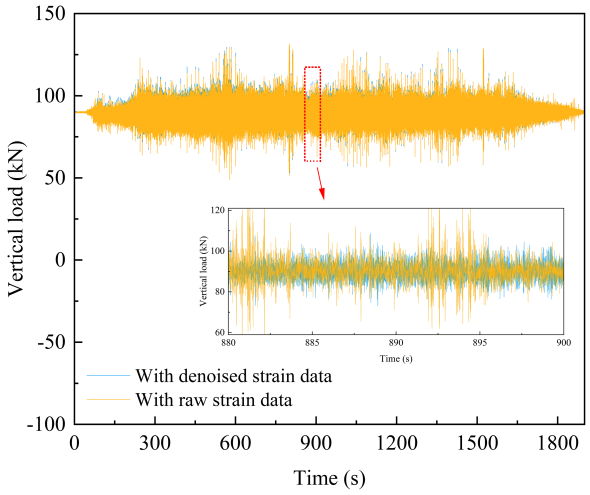


Figure 10: Comparison with the results of the original strain data.

As can be seen from the comparison of results, a large number of impact peaks exist in the load identification results of un-denoised data. Meanwhile, the impact peaks are randomly higher or lower than the true values, and the rising and falling edges are not smooth, accompanied by obvious sawtooth fluctuations. This is attributed to the presence of glitches and power line interference in the raw strain signals, coupled with the amplitude amplification characteristic of the inverse problem, which turns strain glitches with originally small amplitudes into obvious load impacts after inversion. The smoothing capability of Tikhonov regularization is inherently designed to address the ill-posed nature of the inverse problem, serving as a noise suppression measure during the inversion process. Accordingly, procedures such as filtering

and de-spiking act as noise preprocessing methods for response data. Load identification performed on noise-processed response data can minimize noise interference while retaining valid load characteristics.

The improved Tikhonov method is compared with the truncated singular value decomposition (TSVD) method to demonstrate the accuracy of the proposed improved method. The comparison of load identification results is presented in Fig. 11.

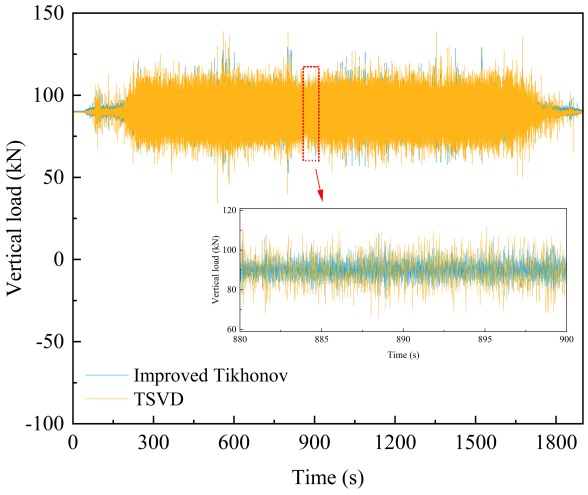


Figure 11: Comparison with the results of the TSVD method.

Both the TSVD method and the Tikhonov method are classical approaches for solving load identification problems. As shown in Fig. 11, the trend of the load results obtained by the improved Tikhonov method is highly consistent with that of the TSVD method. For this segment of test data, the mean relative error (MRE) between the two sets of results is 1.2%, which effectively verifies the accuracy of the load results derived from the improved Tikhonov method. Owing to the large number of data points, a relatively small MRE value is obtained after averaging calculation. When the local data in the time range of 880 s to 900 s are compared, systematic differences in multiple aspects are exhibited in the load identification results due to the discrepancies between the two methods. Such differences originate from the distinct filtering mechanisms applied to singular value components.

In the TSVD method, the first k largest singular value components are retained, while singular components below the truncation threshold are completely discarded, resulting in the total loss of weak load components. As a result, obvious oscillatory waveforms appear at positions of abrupt load changes. Meanwhile, the performance of TSVD is greatly influenced by the truncation order. Under high noise levels, an excessively large truncation order will lead to severe high-frequency noise oscillation in the solution, whereas an excessively small truncation order will cause excessive loss of valid signals. Therefore, the truncation order has to be determined through multiple trials in practical applications of the TSVD method.

In contrast, Tikhonov regularization attenuates all singular components in proportion to the magnitude of their singular values. Small singular value components are not completely eliminated; instead, they are progressively attenuated as the singular values decrease, so that weak load information can be partially preserved. Accordingly, the noise suppression of the Tikhonov regularization method is progressive: the smaller the singular value, the stronger the suppression of noise amplification, leading to a smoother overall noise distribution without abrupt noise surges. Under high-noise environments, the stability of the solution is generally significantly superior to that of the TSVD method.

4.2 Verification of Time-Domain Load Spectra

Based on field measured data from the line, response signals from the section at an operating speed of 250 km/h are selected, and load identification is carried out using the improved Tikhonov regularization method mentioned above. After accounting for the response components of the measuring points under static loading of the bogie frame, the time-domain histories of the seven load components are obtained, as shown in Fig. 12.

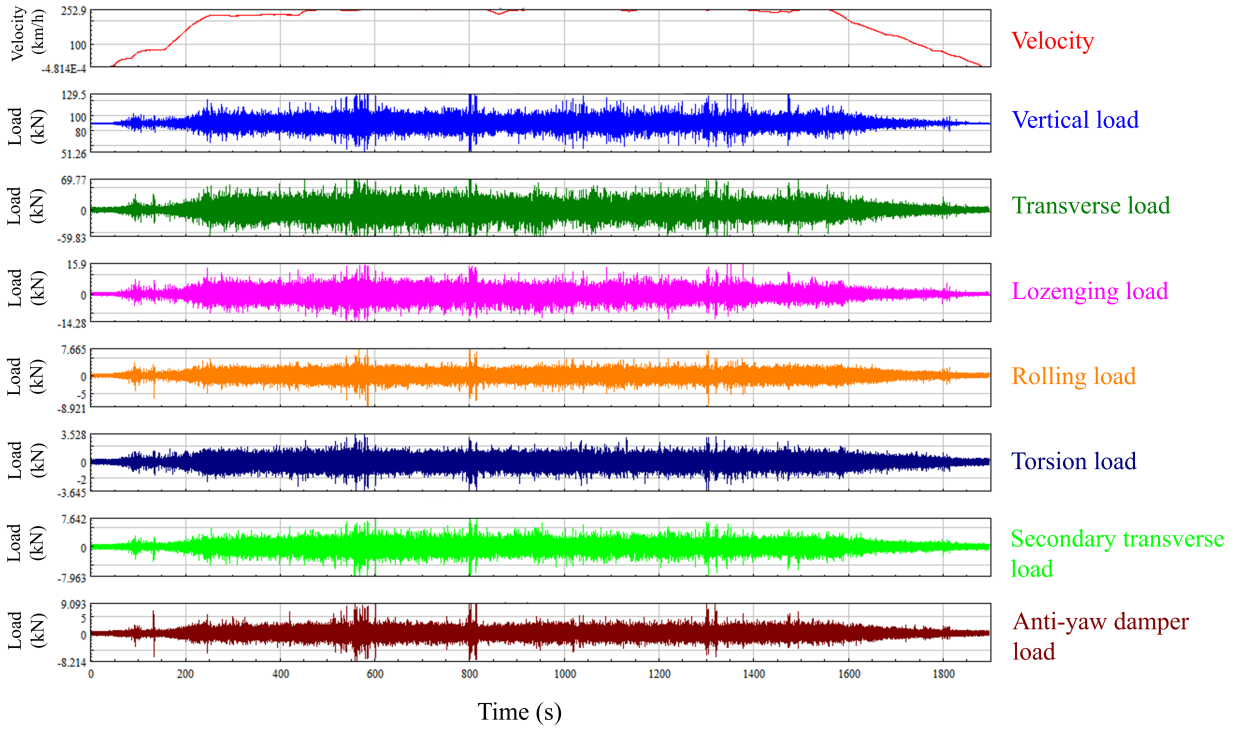


Figure 12: Load identification results.

It can be seen from the load results that vertical load and transverse load have relatively large magnitudes, while the remaining load components exhibit much smaller values. This is because vertical and transverse loads act as the core load-bearing paths of the bogie. They transmit car body weight and wheel-rail forces, and guarantee the structural strength and load-bearing capacity of the frame. In contrast, lozenging load, rolling load and various damper loads are additional loads induced by vibration damping or structural deformation. Owing to their limited action displacement, their amplitudes are far smaller than those of the main load components.

The data obtained from load identification is dynamic, random, and voluminous, so it cannot be used directly. By extracting the maximum values of the loads, the identified load results are compared and verified with the ultimate loads specified in the EN 13749 standard, so as to further clarify the differences between the measured loads and the standard loads. The comparison results are listed in Table 2.

The loads specified in EN 13749 are ultimate design loads with sufficient safety margin, calculated under severe conditions such as full passenger load, extreme acceleration and deceleration, and extreme impact loads. The loads identified in this paper correspond to the actual daily operating loads of the vehicle rather than extreme working conditions, so the overall load level is lower. The measured maximum values of all load components do not exceed the limit values specified in EN 13749, and the load utilization rates fall within

the safe range, indicating that the structure has sufficient strength margin. Among them, the limit utilization rates of rolling loads and anti-yaw damper loads are relatively low, while those of vertical and transverse loads are relatively high, yet still far below the safety limits. Thus, the structure of the bogie frame meets the requirements of ultimate strength verification.

Table 2: Comparative analysis of maximum load values.

Frame Load Systems	Maximum Loads of Measurement (kN)	Ultimate Design Loads of Standard (kN)	Utilization Rate
Vertical load	129.5	196.4	66%
Transverse load	69.8	131.2	53%
Lozenging load	15.9	44.6	36%
Rolling load	7.7	75.4	10%
Torsion load	3.5	9.2	38%
Secondary transverse load	7.6	19.0	40%
Anti-yaw damper load	9.1	46.0	20%

The load signal is processed via rainflow counting to obtain the amplitude and mean value of each load cycle over the entire time domain, and the equivalent load is further calculated accordingly. Based on the principle of damage consistency, the equivalent load reflects the comprehensive effect of load cycles with different amplitudes and occurrence frequencies [36]. The calculation formula of the equivalent load is as follows:

$$F_{eq} = \left[\frac{L}{L_1 N} \sum_{i=1}^{p} n_i F_i^m \right]^{\frac{1}{m}} \tag{16}$$

where, L is the total operational mileage of the bogie under measurement within its specified service life, L_1 is the operational mileage during the bogie field measurement, n_i is the number of cycles corresponding to the load level i obtained using the rainflow counting method, P stands for the series of rainflow counts, m is the S-N curve index, N is the number of cycles corresponding to the fatigue allowable stress.

Comparison of equivalent loads can reflect the actual fatigue load characteristics of the bogie frame during service. The line operation loads obtained from load identification results are compared with standard loads, and the results are presented in Table 3.

The EN 13749 standard is formulated based on European railway line conditions, which feature numerous small-radius curves, a high proportion of curved sections and moderate track smoothness. In contrast, China's high-speed railways are dominated by long straight sections and large-radius curves with high-precision track smoothness. Wheel-rail transverse impact and vertical vibration excitation are thus significantly reduced, resulting in obviously lower transverse and vertical loads than the standard levels. The torsional load and secondary transverse damper load are close to the standard values, which is consistent with the designed unloading characteristics of dampers. The anti-yaw damper load and roll load are relatively low, indicating small amplitudes of vehicle roll and yaw motions in actual operation and a well-performing suspension system.

Table 3: Comparative analysis of equivalent load values.

Frame Load Systems	Equivalent Loads of Measurement (kN)	Ultimate Design Loads of Standard (kN)	Utilization Rate
Vertical load	74.4	140.3	53%
Transverse load	62.9	83.4	75%
Lozenging load	12.7	16.7	76%
Rolling load	6.9	24.8	28%
Torsion load	3.3	5.5	60%
Secondary transverse load	6.0	11.4	53%
Anti-yaw damper load	7.5	27.6	27%

Based on the load characteristics analyzed above, the maximum measured value and equivalent value of each load component do not exceed the limits specified in the EN 13749 standard. The structure has sufficient strength margin, and the calculation results can provide load input for fatigue strength analysis. It is worth noting that the validity of the comparison against the EN 13749 standard in this study is only applicable to conservative estimation in engineering applications. Although the absolute accuracy of the load identification results has not been verified against true reference values, the identified loads are suitable for use in structural strength assessment. Since the actual in-service loads of the bogie frame have not been independently measured, this issue should be given high priority in subsequent research.

5 Engineering Application

In the engineering practice of bogie frame fatigue assessment, traditional assessment workflows suffer from cumbersome operations and redundant procedures, and are prone to result deviations due to the large volume of calculations involved. Moreover, accurate load boundary conditions are helpful to carry out accurate structural fatigue assessment. Therefore, it is necessary to implement the "load identification–fatigue assessment" integrated procedure in the form of a visual software. A visualization software is developed to meet the practical engineering requirements of multiaxial fatigue assessment for vehicle bogie frames, which covers the entire workflow from finite element result reading, multiaxial stress calculation, and material parameter configuration to result visualization. The software adopts a modular three-layer architecture, namely the presentation layer, logic layer and computing layer.

(1) Presentation layer

The presentation layer provides a human-computer interaction interface. The interactive interface is designed based on the PyQt5 graphical interface framework [37], which offers users concise and intuitive operation entries and converts the professional fatigue assessment workflow into visual operations. It mainly includes interfaces for loading file reading, multiaxial stress calculation, Goodman curve parameter configuration and plotting, as well as multi-set result display. All interface modules are rationally arranged and connect the entire fatigue assessment workflow.

(2) Logic layer

The logic layer encapsulates the multiaxial stress algorithm and the Goodman criterion. It receives operation instructions from the user interaction layer, dispatches underlying computing layer modules to execute tasks, and simultaneously completes data circulation, processing and management. Its main functions are as follows: instruction parsing and workflow scheduling to ensure the orderly operation of each module following the standard fatigue assessment procedure; data parsing, filtering and format conversion

to realize data adaptation between different modules; caching and management of parameters and results to improve platform operation efficiency and provide data support for subsequent result display and export.

(3) Computing layer

The computing layer is responsible for the parsing and storage of finite element results and implements algorithms related to fatigue assessment. Its main functions include extracting the original stress data required for fatigue calculation, solving the multiaxial stress at evaluation points, ensuring the stable operation of the platform, and providing timely feedback on abnormal conditions during the calculation process.

The calculation result interface of the software is shown in Fig. 13.

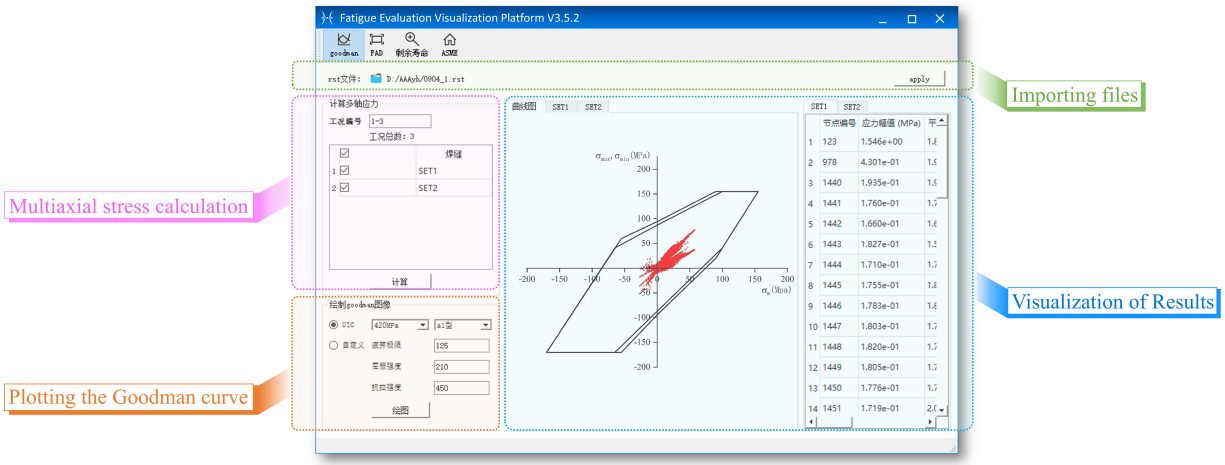


Figure 13: Visualization of fatigue evaluation.

The finite element model of the bogie frame is established through structural discretization using Solid185 solid elements and Shell181 shell elements. The material parameters are determined based on the data obtained from tensile tests. Considering the actual structure, computational workload and calculation accuracy of the bogie frame, a mesh element size of 10 mm is selected. The final model comprises a total of 207,936 elements and 77,967 nodes. The steel springs at the bogie axle ends are simulated with COMBIN14 elements, while motors and other suspended components are modeled using MASS21 elements.

All seven identified load results mentioned above are incorporated into the finite element calculation. The obtained load identification results are adopted as external excitations. In accordance with their actual action positions and loading directions, these excitations are applied to corresponding positions on the finite element model, including mounting seats and connection points, to calculate the stress state of the bogie frame. The finite element model and the principal stress distribution results under three load cases with different loading directions are shown in Fig. 14. Other load cases are not presented here, as most of them are local loads. The fatigue assessment software developed in this study generates visual assessment results, which intuitively present the distribution of fatigue safety margin across the bogie frame. The relevant results are illustrated in Fig. 15.

It can be seen from the Fig. 13 that all calculated stress points at key assessment nodes under combined load cases are distributed within the envelope of the Goodman curve. No stress point exceeds the curve boundary, and the results meet the design requirements. This analysis verifies the fatigue reliability of the bogie frame under identified loads and confirms the applicability of the visualization system in practical engineering, establishing a methodological system for the service safety assessment of bogie structures.

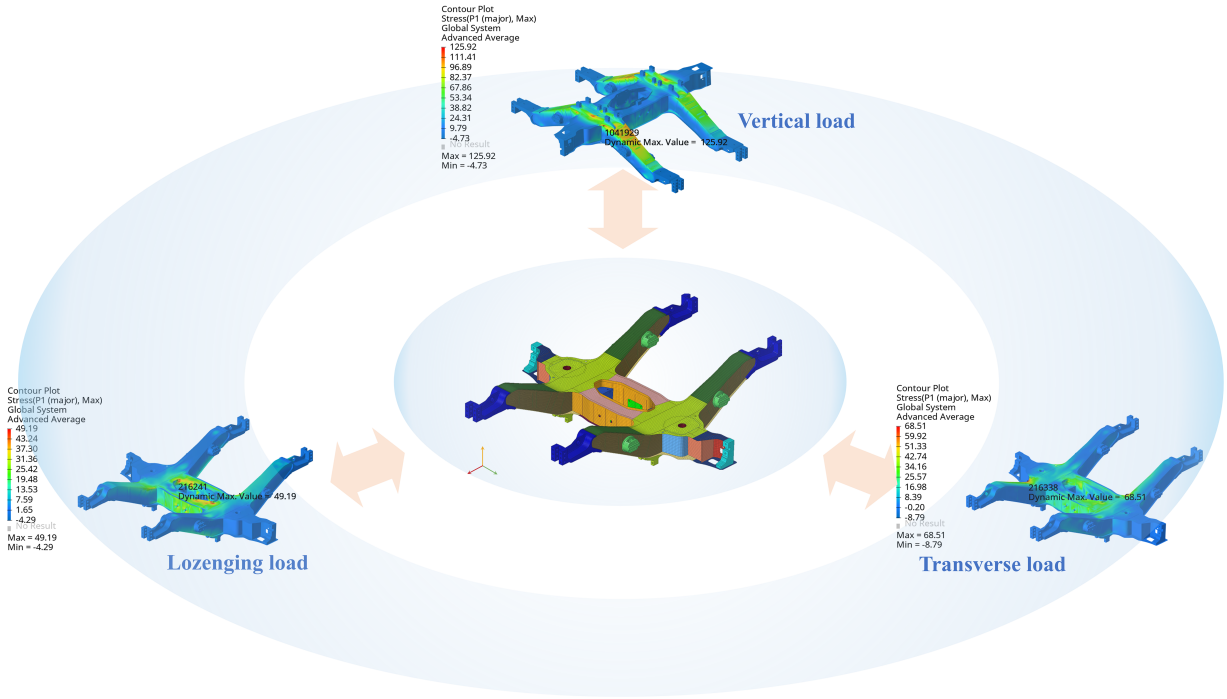


Figure 14: Finite element model and simulation results.

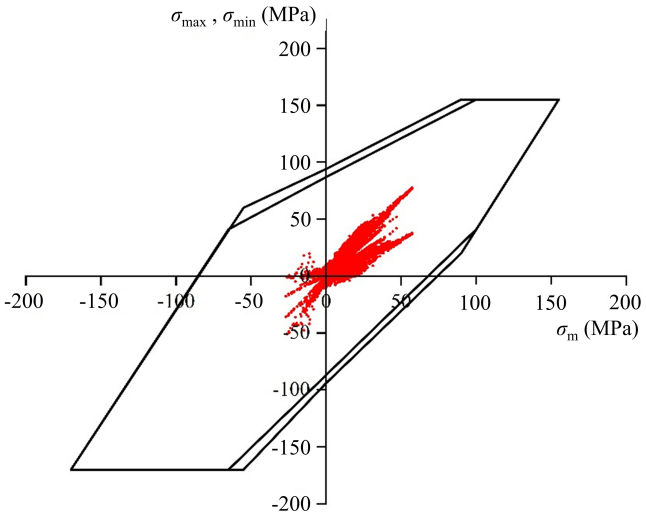


Figure 15: Results of fatigue evaluation.

6 Conclusion

An improved method based on standard Tikhonov regularization is proposed by combining intelligent algorithms and physical models, to address the issue that weakly correlated loads associated with small singular values are considerably susceptible to noise interference in bogie frame load identification. A systematic procedure for load identification and fatigue assessment of the bogie frame is established. Furthermore, the accuracy of the proposed method is further validated using field measurement data of a new-type bogie frame with inner axle-boxes. This study provides a solution for bogie frame load

identification, and is of great value to the structural strength design and safety assessment of railway vehicles. The conclusions are summarized as follows:

(1) This method introduces a non-identity matrix constructed from the singular values of the transfer coefficient matrix and adopts a genetic algorithm for adaptive parameter selection. Minor corrections are applied to large singular values associated with strongly correlated loads, while the correction magnitude for small singular values corresponding to weakly correlated loads that are sensitive to noise is increased. Through such differentiated processing of response data, the accuracy of bogie frame load identification is improved. Compared with the standard Tikhonov method, both the standard deviation and the mean relative error of the improved algorithm are significantly reduced.

(2) The comparison with the EN 13749 standard indicates that the load results of this study are suitable for conservative estimates in engineering applications. In accordance with the requirements of the EN 13749 standard for bogie load analysis, comparisons are conducted from two perspectives: ultimate load and equivalent load. The maximum measured values and equivalent loads of each load component do not exceed the ultimate limits and simulated service loads specified in the standard, and all load utilization ratios are below 1. The new bogie frame structure has sufficient strength margin, and the calculation results can provide load input for fatigue strength analysis.

(3) The method proposed in this study is developed into visualization software and applied to the fatigue assessment of the new-type bogie frame with inner axle-boxes. The extreme values of the obtained load identification results are taken as external excitations and applied to the finite element model of the bogie frame according to the actual action positions and loading directions. The fatigue calculation is performed using the fatigue assessment software developed in this paper, and visual assessment results are generated. All calculated stress points at key assessment nodes under combined load cases are distributed within the envelope of the Goodman curve. No stress point exceeds the curve boundary, which satisfies the design requirements. This analysis verifies the fatigue reliability of the bogie frame under identified loads and confirms the applicability of the visualization system in practical engineering.

Owing to the diverse loads acting on the bogie and the constraints of field measurement conditions, future research focuses on decoupling analysis for other loads and comparative validation against load values measured by high-precision sensors.

Acknowledgement: Not applicable.

Funding Statement: The work is supported by the Science and Technology Research and Development Program Project of China National Railway Administration Group (RJ2025J001), the Research Project of China National Railway Administration Group (SJ2024-024), the Doctoral Research Initiation Program Project of Liaoning Province Natural Science Foundation (2025-BS-0452), and the Basic Science Research Project of Liaoning Provincial Department of Education (JYTMS20230039).

Author Contributions: The authors confirm contribution to the paper as follows: study conception and design: Bo Liu, Yuedong Wang, Jiaqi Zhang; data collection: Tao Guo, Guojie Cai, Yawen Fu; analysis and interpretation of results: Bo Liu, Qi Dong, Qiyu An; draft manuscript preparation: Bo Liu, Jiaqi Zhang. All authors reviewed and approved the final version of the manuscript.

Availability of Data and Materials: Data will be made available on request.

Ethics Approval: Not applicable.

Conflicts of Interest: The authors declare no conflicts of interest.

Nomenclature

$\boldsymbol{A}$	Load transfer coefficient matrix
α	Power adjustment parameter
ADL	Anti-yaw damper load
$\boldsymbol{b}$	Measurement response matrix
EMU	Electric multiple unit
f	Filter function
GCV	Generalized cross-validation
$\boldsymbol{I}$	Identity matrix
λ	Regularization parameter
$\boldsymbol{L}$	The standard Tikhonov regularization matrix
$\boldsymbol{L_I}$	The improved Tikhonov regularization matrix
L	The total operational mileage within service life
L_1	The operational mileage under measurement
LL	Lozenging load
MRE	Mean relative error
m	The S-N curve index
N	The number of cycles corresponding to the fatigue allowable stress
n_i	The number of cycles corresponding to level i
P	The series of rainflow counts
RE	Relative error
RL	Rolling load
STL	Secondary transverse load
SVD	Singular value decomposition
SD	Standard deviation
σ_i	The singular values
$\sigma_{\max}$	Maximum stress
$\sigma_{\min}$	Minimum stress
σ_{m}	Average stress
ToL	Torsion load
TSVD	Truncated singular value decomposition
U	The $m \times m$ orthogonal matrices
u_i	The eigenvectors obtained from AA^{T}
V	The $n \times n$ orthogonal matrices
v_i	The eigenvectors obtained from $A^{\mathrm{T}}A$
$\boldsymbol{x}$	Load matrix
VL	Vertical load
$\sum$	The diagonal matrix
γ_i	The singular values obtained from the singular value decomposition

References

1. Luo W, Wang B, Wang W, Li Q, Qian G. Fatigue failure mechanism of metro bogie frames under P2 resonance and track stiffness variation. Eng Fail Anal. 2026;186:110503. doi:10.1016/j.engfailanal.2025.110503.
2. Jiang JH, Zhang F. Research progress on structural dynamic load identification. J Vibr Eng. 2024;37(10):1625–50. (In Chinese). doi:10.16385/j.cnki.issn.1004-4523.2024.10.001.
3. Li L, Wang B, Wang W, Wang H. A method for constructing the load spectrum of metro bogie frame for fatigue damage prediction. Measurement. 2025;247(4):116790. doi:10.1016/j.measurement.2025.116790.
4. Paulo E, Vieira FS, Araújo AL. Fatigue analysis of a freight wagon bogie frame using a hybrid peridynamic-finite element submodeling approach. Eng Fract Mech. 2026;345(5–6):112512. doi:10.1016/j.engfracmech.2026.112512.

5. Ji C, Sun S, Li Q, Wang W, Ren Z, Yang G. A novel method for the general application of measured load spectra to different high-speed train bogie frames based on virtual track irregularity. Measurement. 2022;198:111369. doi:10.1016/j.measurement.2022.111369.
6. Zhu T, Wang XR, Fan YW, Wang MM, Zhang JK, Xiao SN, et al. A time domain method for wheel-rail force identification of rail vehicles. Veh Syst Dyn. 2022;60(3):790–809. doi:10.1080/00423114.2020.1838562.
7. Zhu T, Wu JX, Wang XR, Xiao S, Yang GW, Yang B. Time domain identification and comparison of vertical wheel-rail force of rail vehicles and its machine learning correction. Chin J Theor Appl Mech. 2024;56(1):247–57. (In Chinese).
8. Ren LH, Zhou RS, Ji YJ, Zeng JW. Radial tire load identification model of straddle-type monorail vehicle based on concatenated deep neural network. China Railw Sci. 2025;46(1):136. doi:10.3969/j.issn.1001-4632.2025.01.12.
9. Lu P, Han L, Wang X, Yang D, Hou Y. Dynamic load identification of metro bogie frame based on the strain signals and modal parameters. Mech Syst Signal Process. 2025;237(2):113098. doi:10.1016/j.ymssp.2025.113098.
10. Guo J, Zhang G, Shi H, Zeng J. Small-amplitude bogie hunting identification method for high-speed trains based on machine learning. Veh Syst Dyn. 2024;62(5):1253–67. doi:10.1080/00423114.2023.2224906.
11. Huang Y, Cui B, Mao X, Yang J. Prior knowledge-informed graph neural network with multi-source data-weighted fusion for intelligent bogie fault diagnosis. Machines. 2024;12(12):838. doi:10.3390/machines12120838.
12. Sun Y, Luo L, Chen K, Qin X, Zhang Q. A time-domain method for load identification using moving weighted least square technique. Comput Struct. 2020;234(5):106254. doi:10.1016/j.compstruc.2020.106254.
13. Xu G, Weng Z, Gan J, Liu H, Wu W. Shape function method of Tikhonov regularization for vertical bending moment identification based on parameter updating. Measurement. 2025;242:116190. doi:10.1016/j.measurement.2024.116190.
14. Xi ZY, Yan YJ, Chang XT. Optimization method of dynamic load identification based on genetic algorithm. J Mech Strength. 2015;37(4):593–7. (In Chinese). doi:10.16579/j.issn.1001.9669.2015.04.001.
15. Pacheco CC, Lacerda CR, Colaço MJ. A GSVD-based methodology for automatic selection of high-order regularization parameters in inverse heat conduction problems. Int Commun Heat Mass Transf. 2025;163(11):108684. doi:10.1016/j.icheatmasstransfer.2025.108684.
16. Wang L, Gu W. A-optimal design method to determine the regularization parameter of coseismic slip distribution inversion. Geophys J Int. 2019;221(1):440–50. doi:10.1093/gji/ggaa030.
17. Jing W, Jiang JH, Xu F, Bao HY, Chen S. Multi-point stationary random load identification method based on improved regularization. J Vib Meas Diagn. 2025;45(2):219. doi:10.16450/j.cnki.issn.1004-6801.2025.02.002.
18. Xiu R, Spiryagin M, Wu Q, Yang S, Liu Y. Fatigue life assessment methods for railway vehicle bogie frames. Eng Fail Anal. 2020;116(1):104725. doi:10.1016/j.engfailanal.2020.104725.
19. Wang BJ, Li Q, Ren ZS, Sun SG. Improving the fatigue reliability of metro vehicle bogie frame based on load spectrum. Int J Fatigue. 2020;132:105389. doi:10.1016/j.ijfatigue.2019.105389.
20. Yin Y, Jiang S, Li Q, Wang B, Hu H, Guo L. Research on the establishment of load spectrum for fatigue damage assessment of high-speed train bogie frame. Measurement. 2025;251(1):117080. doi:10.1016/j.measurement.2025.117080.
21. Li J, Ren Z, Wu Y, An R. Fatigue damage assessment of high-speed train bogie frame load spectra based on phase reconstruction. Eng Fail Anal. 2024;159:108008. doi:10.1016/j.engfailanal.2024.108008.
22. Zhang Y, Lu Y, Yan B, Xue S, Wang Q, Liu X. Optimal sensor placement for railway vehicle bogie frame based on strain modal analysis. Measurement. 2025;253(6):117466. doi:10.1016/j.measurement.2025.117466.
23. Guo T, Chen B, Liu B, Wang YD, Zhang J, Dong Q, et al. Research on load characteristics of high-speed train bogie frame with inner axle-box based on measurement data. Int J Struct Integr. 2026;17(5):1020–42. doi:10.1108/ijsi-09-2025-0245.
24. Li P, Zhao D, Li L. Truncated SVD and Tikhonov regularization united algorithm to solve the ill-conditioned equation in muon positioning system. Adv Space Res. 2025;76(8):4621–34. doi:10.1016/j.asr.2025.07.048.
25. Liu J, Jiang W, Luo Z, Zhang P, Yang L, Cheng Y, et al. The application of piecewise regularization reconstruction to the calibration of strain beams. Sensors. 2024;24(9):2744. doi:10.3390/s24092744.

26. Gao J, Zhang Z, He Y, Liu J, Li Y. Operational transfer Path analysis based on Tikhonov regularization and particle swarm optimization algorithm. J Vibr Control. 2025;31(19–20):4300–14. doi:10.1177/10775463241285472.
27. Mabrouk M, Ning P, Zheng D, Wang T, Wu H, Altabey WA, et al. Optimizing gear NVH performance using genetic algorithm-based on tooth profile modification and a comparative analysis of simulation and experimental outcomes. Measurement. 2026;258(3):119163. doi:10.1016/j.measurement.2025.119163.
28. Zhang Z, He Z, Yang B, Wang Y, Xiao S, Hou M, et al. An improved Goodman-Smith fatigue limit diagram for railway vehicle base metals and welded structures. Int J Fatigue. 2024;182(7):108160. doi:10.1016/j.ijfatigue.2024.108160.
29. Tang Y, Wang Y, Liu J, Tian B, Dong Q, He Z, et al. A method for modifying octagonal Goodman–Smith fatigue limit diagram. Int J Struct Integr. 2024;15(2):343–59. doi:10.1108/ijsi-12-2023-0136.
30. Zhang D, Li Y, Fu Z, Wang Y, Xu K. Fatigue reliability analysis of bogie frames considering parameter uncertainty. Int J Fatigue. 2025;190(11):108632. doi:10.1016/j.ijfatigue.2024.108632.
31. BS EN 13749. Railway applications—wheelsets and bogies method of specifying the structural requirements of bogie frames. London, UK: British Standards Institution; 2011.
32. Ji C, Gao Y, Liu Z, Yang G. Field measurement and characteristics analysis of transverse load of high-speed train bogie frame. Machines. 2025;13(10):905. doi:10.3390/machines13100905.
33. Dong Q, Wang Y, Zhang J, Liu B, Guo T, Hou M. Impact of wheel tread damage-induced vibrational loads on the service life of rail bogie frames. Eng Fail Anal. 2025;176:109630. doi:10.1016/j.engfailanal.2025.109630.
34. Guo T, Chen B, Wang Y, Cai G, Hou M, Dong Q. Vibration characteristics and fatigue performance of bogie frame with inner axle box for high-speed trains. Machines. 2025;13(11):1056. doi:10.3390/machines13111056.
35. GB/T 228.1. Metallic materials—tensile testing-Part 1: method of test at room temperature. Beijing, China: China Iron & Steel Association; 2016.
36. Wu Y, Ren Z. Fatigue damage assessment of a metro vehicle bogie frame based on measured field load. Machines. 2025;13(4):306. doi:10.3390/machines13040306.
37. de Oliveira I, Corgozinho AL, Rocha H, Valente MT. Property-based testing in Python: empirical insights. Empir Softw Eng. 2026;32(1):30. doi:10.1007/s10664-026-10953-w.